Chronic administration of cholesterol oximes in mice increases transcription of cytoprotective genes and improves transcriptome alterations induced by alpha-synuclein overexpression in nigrostriatal dopaminergic neurons

Franziska Richter[1], **Fuying Gao**[2], **Vera Medvedeva**[1], **Patrick Lee**[1], **Nicholas Bove**[1], **Sheila M. Fleming**[1], **Magali Michaud**[3], **Vincent Lemesre**[1], **Stefano Patassini**[1], **Krystal De La Rosa**[1], **Caitlin K. Mulligan**[1], **Pedrom Sioshansi**[1], **Chunni Zhu**[1], **Giovanni Coppola**[1,2], **Thierry Bordet**[3], **Rebecca Pruss**[3], and **Marie-Françoise Chesselet**[1]

[1]Department of Neurology, The David Geffen School of Medicine at UCLA, 710 Westwood Plaza, Los Angeles, CA 90095-1769, USA

[2]Department of Psychiatry, Semel Institute for Neuroscience and Human Behavior, The David Geffen School of Medicine at UCLA, 710 Westwood Plaza, Los Angeles, CA 90095-1769, USA

[3]Trophos S.A., Parc Scientifique de Luminy, Case 931, 13288 Marseille Cedex 9, France

Abstract

Cholesterol-oximes TRO19622 and TRO40303 target outer mitochondrial membrane proteins and have beneficial effects in preclinical models of neurodegenerative diseases leading to their advancement to clinical trials. Dopaminergic neurons degenerate in Parkinson's disease (PD) and are prone to oxidative stress and mitochondrial dysfunction. In order to provide insights into the neuroprotective potential of TRO19622 and TRO40303 for dopaminergic neurons in vivo, we assessed their effects on gene expression in laser captured nigrostriatal dopaminergic neurons of wildtype mice and of mice that over-express alpha-synuclein, a protein involved in both familial and sporadic forms of PD (Thy1-aSyn mice). Young mice were fed the drugs in food pellets or a control diet from 1 to 4 months of age, approximately 10 months before the appearance of striatal dopamine loss in this model. Unbiased weighted gene co-expression network analysis (WGCNA) of transcriptional changes revealed effects of cholesterol oximes on transcripts related to mitochondria, cytoprotection and anti-oxidant response in wild-type and transgenic mice, including increased transcription of stress defense (e.g. *Prdx1, Prdx2, Glrx2, Hspa9, Pink1, Drp1, Trak1*) and dopamine-related (*Th, Ddc, Gch1, Dat, Vmat2, Drd2, Chnr6a*) genes. Even at this young age transgenic mice showed alterations in transcripts implicated in mitochondrial function and oxidative stress (e.g. *Bcl-2, Bax, Casp3, Nos2*), and both drugs normalized about 20% of these

Correspondence: Marie-Françoise Chesselet, M.D., Ph.D., Department of Neurology, The David Geffen School of Medicine at UCLA, 710 Westwood Plaza, Los Angeles, CA 90095-1769, 310-267-1782, 310-267-1786 (fax), mchesselet@mednet.ucla.edu.

alterations. Young Thy1-aSyn mice exhibit motor deficits that differ from parkinsonism and are established before the onset of treatment; these deficits were not improved by cholesterol oximes. However, high doses of TRO40303 improved olfaction and produced the same effects as dopamine agonists on a challenging beam test, specifically an increase in footslips, an observation congruent with its effects on transcripts involved in dopamine synthesis. High doses of TRO19622 increased alpha-synuclein aggregates in the substantia nigra; this effect, not seen with TRO40303 was inconsistent and may represent a protective mechanism as in other neurodegenerative diseases. Overall, the results suggest that cholesterol oximes, while not improving early effects of alpha-synuclein overexpression on motor behavior or pathology, may ameliorate the function and resilience of dopaminergic neurons in vivo and support further studies of neuroprotection in models with dopaminergic cell loss.

Introduction

Parkinson's disease (PD) causes widespread pathology in brain but it is the progressive dysfunction and death of nigrostriatal dopaminergic neurons that is mainly responsible for the disabling motor deficits characteristic of the disease. Therefore, preserving the function and improving the survival of these dopaminergic neurons remain a therapeutic priority. Oxidative stress and mitochondrial dysfunction have been observed in patients with sporadic Parkinson's disease (PD) (Lin and Beal, 2006; Schapira et al., 1989; Schapira and Jenner, 2011). Mutations that cause rare familial forms of PD affect mitochondria clearance or function (Subramaniam and Chesselet, 2013), and alpha-synuclein, a protein related to both familial and sporadic forms of PD (Hardy, 2010; Pankratz et al., 2009), affects mitochondrial function (Devi et al., 2008; Loeb et al., 2010; Nakamura, 2013). Despite the likely involvement of mitochondria in the disease, previous use of anti-oxidants in PD has been disappointing (Stocchi and Olanow, 2013), however compounds that directly target mitochondria have not been extensively examined.

Cholesterol oximes, a novel family of neuroprotective compounds, were originally identified in a cell-based assay of neurotrophic deprivation in primary motor neurons (Bordet et al., 2007). The lead compound, olesoxime (TRO19622; cholest-4-en-3-one, oxime), provides similar protection to human iPSC-derived motor neurons (Yang et al., 2013) and is active in multiple in vivo models of neurodegeneration (Bordet et al., 2008; Bordet et al., 2007; Magalon et al., 2012; Martin et al., 2011; Sunyach et al., 2012; Xiao et al., 2009; Xiao et al., 2012). TRO40303 (3,5-seco-4-nor-cholestan-5-one oxime-3-ol) was derived from a chemistry optimization program based on the structure of TRO19622 and has pronounced cytoprotective effects and preserves cardiac tissue in a rat model of cardiac ischemia-reperfusion injury (Schaller et al., 2010). These cholesterol oximes access brain after oral administration, are safe, and have moved forward into clinical trials (Le Lamer et al., 2014; Lenglet et al., 2014). They bind to mitochondrial outer membrane proteins, the 18kDa translocator protein (TSPO) and the voltage-dependent anion channel (VDAC, TRO19622 only), reduce oxidative stress-induced mitochondrial permeability transition (mPTP), and the release of pro-apoptotic factors (Bordet et al., 2007; Schaller et al., 2010). Previous studies with TRO compounds have provided evidence for stabilization of mitochondrial

function under different disease conditions (Bordet et al., 2007; de Tassigny et al., 2013; Gouarne et al., 2013).

The goals of the present study were 1): to examine the molecular effects of cholesterol oximes on dopaminergic neurons; and 2) test their ability to reverse alpha-synuclein induced gene alterations in these neurons. We have used a well-characterized mouse model of alpha-synuclein over-expression in which full-length, human, wild-type alpha-synuclein is expressed under the Thy-1 promoter (Thy1-aSyn mice; Chesselet et al., 2012; Rockenstein et al., 2002). The Thy1-aSyn mice show a loss of striatal dopamine by 14 months, providing a long window of time to assess the molecular mechanisms that may lead to nigrostriatal pathology. We used young adult wildtype mice and Thy1-aSyn littermates as a cost-effective initial approach to study the effects of chronic administration of cholesterol oximes on dopaminergic neurons under physiological versus disease condition. TRO19622 or TRO40303 or a control diet were administered in food pellets to wild type mice or to Thy1-aSyn mice from 1 to 3 months of age. We assessed behavioral and pathological effects of alpha-synuclein over-expression observed at this early age in Thy1-aSyn mice (Chesselet et al., 2012), followed by an analysis of transcriptional changes in laser captured nigrostriatal dopaminergic neurons. At a dose that reached expected pharmacologically active levels in brain based on in vitro studies, TRO40303 had a marked effect on transcripts involved in neuroprotection and dopamine synthesis in wild-type mice, and to a lesser extent, in Thy1-aSyn mice. Although they did not improve early behavioral and pathological effects of alpha-synuclein over-expression, both compounds normalized a significant fraction of transcript changes in transgenic mice, with TRO40303 having the stronger effect.

Materials and Methods

Mice

Animal care was conducted in accordance with the United States Public Health Service Guide for the Care and Use of Laboratory Animals, with approval by the Institutional Animal Care and Use Committee at the University of California Los Angeles (UCLA). Wildtype mice were littermates of transgenic mice overexpressing human wildtype alpha-synuclein under the Thy-1 promoter (Thy1-aSyn) (Rockenstein et al., 2002) maintained on a hybrid C57BL/6-DBA/2 background (Fleming et al., 2004). Only male mice were used in the study (Chesselet et al., 2012). The genotype of all wildtype and Thy1-aSyn mice was determined by polymerase chain reaction (PCR) amplification analysis of tail DNA at three weeks of age and verified at the end of the experiment. Mice enrollment in the study carefully balanced litters across treatment groups and investigators involved in drug administration, data gathering, and data analyses were unaware of genotype and treatment for the duration of the study. Animals were maintained on a reverse light/dark cycle with lights off at 10 am and all testing was performed between 1–4 pm during the dark cycle under low light. Food and water were available ad libitum except before and during a 11 days moderate food restriction period at the end of the treatment period for olfactory testing. To insure that food restriction during the drug treatment period did not result in significant drop in plasma and brain levels of TROPHOS (TRO) compounds, we verified that compound levels remain stable in separate groups of mice.

Experimental design

The compounds were administered in food pellets as bioavailability of TRO19622 and TRO40303 per os in mice had been previously shown, and low and high dosages for each compound were chosen based on extensive previous in vivo studies for efficiency of both compounds (Bordet et al., 2007; Schaller et al., 2010). We confirmed expected plasma and brain levels in a satellite group of wildtype mice fed over 5 days with the compounds. For per os administration, TRO19622 (60–1280 mg/kg food pellets equivalent to 6–180 mg/kg bodyweight/day) or TRO40303 (70–700 mg/kg food pellets equivalent to 9–70 mg/kg bodyweight/day) were prepared in commercially available mouse food pellets (AIN76-A, BioServ, Frenchtown, NJ). Mice were randomly assigned to 4 treatment groups powered to detect drug effects based on our power analyses (Chesselet et al., 2012) (n=20 per group: wildtype/control, Thy1-aSyn/control, wildtype/drug, Thy1-aSyn/drug) for low and high dose of TRO19622 and TRO40303, respectively. Mice were allowed free access to the food (either control or drug-enriched food pellets) for 3 months beginning at 1 month of age. General condition, body weight and food intake was recorded daily over the treatment period. Body temperature was recorded weekly. Motor deficits on the challenging beam and pole were assessed after 1 and 3 months of drug administration, in the cylinder and in an olfactory (buried pellet) test after 1 and 2 months of administration, respectively, following our previously published protocols (Fleming et al., 2011).

After 3 months of treatment, i. e. at 4 months of age, a pre-determined subset of animals from the high TRO compound dosages and respective control groups were sacrificed and one hemisphere of their brains used for gene expression analysis (see *Transcriptome analysis* below).

Plasma and brain (one hemisphere) drug levels were determined in half of each group of cholesterol-oxime treated mice at the end of treatment. Two additional satellite groups of wildtype and Thy1-aSyn mice were used to determine plasma and brain levels after 1 or 2 months of treatment. In addition, in separate groups of mice, we validated that moderate food restriction over 11 days during the buried pellet test for olfactory function does not result in significant changes in the plasma and brain levels of the drug in all treatment groups (data not shown). Samples were stored at −80°C. Concentrations of TRO compounds were determined by high-performance liquid chromatography with tandem mass spectrometry detection (Bordet et al., 2007; Schaller et al., 2010).

The remaining animals were deeply anesthetized with pentobarbital (100 mg/kg, ip) and perfused through the heart with 0.1M phosphate buffered saline (PBS) at room temperature followed by 4% paraformaldehyde. Their brains were processed for alpha-synuclein immunohistochemistry and quantitative assessment of proteinase-K resistant alpha-synuclein aggregates in the substantia nigra according to our previously published protocols (Fleming et al., 2011). Quantification was only performed on tissue from transgenic mice because wildtype mice do not develop proteinase K-resistant aggregates of alpha-synuclein. The contour of the substantia nigra was delineated at 5X objective in 2 sections per mouse (stereo investigator software, MicroBrightField, Colchester, VT, coupled to a Leica DM-LB microscope with a Ludl XYZ motorized stage and z-axis microcator MT12, Heidenheim,

Traunreut, Germany). The contour was then divided in 4 subregions as shown in Fig. S1. Images of four subregions of the substantia nigra were then acquired using the same software and 40x objective (one image per subregion). Images of the substantia nigra from both hemispheres were transformed to 8 bit files using ImageJ software (ImageJ software, version 1.38x, National Institutes of Health). In order to perform the particle analysis in ImageJ the threshold was set manually to ensure the inclusion of all aggregates. The diameters of aggregates assessed ranged from 1 μm – 30 μm. Inclusions were defined by circularity to avoid inclusion of dust or other artifacts. The number of aggregates was calculated per 100 μm^2 and the surface area covered by aggregates was measured using ImageJ.

Transcriptome analysis of isolated TH positive neurons in the substantia nigra

For preparation of tissue for RNA analysis a subset of mice having received control food or food containing the high (pharmacologically active) dose of the cholesterol oximes, were deeply anaesthetized with pentobarbital (100 mg/kg) and perfused briefly with phosphate buffered saline (PBS) to remove blood. Brains were removed rapidly and the two hemispheres were dissected. One hemisphere was quickly frozen on powdered dry ice for drug level analysis. The other hemisphere was snap frozen in –30°C 2-methylbutane for gene expression analysis. Snap frozen brains from the following groups were used for transcriptome analysis (n=5 each): wildtype + control, wildtype + TRO19622, Thy1-aSyn + control, Thy1-asyn + TRO19622; wildtype + control, wildtype + TRO40303, Thy1-aSyn + control, Thy1-asyn + TRO40303. For laser-capture microdissection (LCM) of TH-positive neurons, the substantia nigra was cut in 10 μm serial coronal sections and quickly immunostained for TH as described previously (Meurers et al., 2008; Richter et al., 2009) with adaptation for immunofluorescent staining as follows: following ethanol fixation for 1 minute, sections were incubated with a primary antibody recognizing TH (rabbit anti TH, 1:200, Millipore, Billerica, MA) for 2 minutes followed by incubation for 2 minutes in Cy3 conjugated goat anti-rabbit secondary antibody (1:200, Vector Laboratories, Burlingame, CA) on ice. Sections were rinsed in sterile ice-cold 1x PBS between each incubation step. Finally, sections were dehydrated in ethanol and incubated in xylene for 5 minutes. The entire procedure was carried out under RNase-free conditions. Duplicate samples of 250 TH-positive neurons (500 total) were collected from each mouse (Fig. 1A–C). RNA extraction and T7-based mRNA amplification (Kamme et al., 2004; Meurers et al., 2008; Richter et al., 2009) were performed using manufactured kits (TargetAmp™ 2-Round Biotin-aRNA Amplification Kit 3.0, Epicentre, Illumina, Wisconsin, USA). Dopaminergic phenotype and the purity of samples obtained with this technique were verified via gel electrophoresis of polymerase chain reaction (PCR) products from Th, Gad1 (GABAergic neuron marker), Gfap (astroglia marker) and Hprt (housekeeping gene) mRNAs as show in Fig. 1D. Quality of amplified RNA was assessed using an Agilent Bioanalyzer. Amplified RNA was labeled and hybridized to Illumina Mouse Ref 8 v2.0 gene expression BeadChips, querying the expression of approximately 25,600 RefSeq-curated gene targets, for microarray analysis by the Southern California Genotyping Consortium (SCGC) Core using the Illumina BeadStation platform.

Statistical microarray analysis and gene expression analysis was performed at the Informatics Center for Neurogenetics and Neurogenomics (ICNN) core at UCLA using R (www.r-project.org) and Bioconductor (www.bioconductor.org10) packages as described (Coppola, 2011; Coppola et al., 2008), and Weighted Gene Coexpression Network Analysis (WGCNA) (Konopka et al., 2009; Zhang and Horvath, 2005). Briefly, genes consistently present on arrays, with high coefficient of covariation and high connectivity were selected for network construction and were hierarchically clustered and modules determined based on their topological overlap using a dynamic tree-cutting algorithm (http://www.genetics.ucla.edu/labs/horvath/CoexpressionNetwork/). VisANT was used to visualize modules (http://visant.bu.edu/). Gene ontology analysis was performed using the DAVID functional annotation tool (http://david.abcc.ncifcrf.gov/). Final functional gene expression analysis and pathway analysis was done using Ingenuity pathway analysis tool (IPA, Ingenuity Systems).

After normalization and correction for batch effect using ComBat (Johnson et al., 2007), gene expression data for TRO19622 and TRO40303 were separately compared to the average of controls from both experiments. Control-treated groups of both TRO compounds could hereby be merged to increase power for statistical analysis (n=10 for each control group, n=5 per group for TRO compound treated groups).

Quantitative real time PCR validation

First-strand cDNA from non-amplified RNA samples from TH positive neurons obtained by LCM was synthesized using the High Capacity cDNA Reverse Transcription Kit (Applied Biosystems, Pleasanton, CA, USA) and random primers according to the manufacturer's protocol. Specific TaqMan Gene expression assays were used with probes that span exons (Applied Biosystems). High efficacy of the respective assay was evaluated by the manufacturer, but specific sequences are proprietary. One μl of cDNA was added to TaqMan Universal Master Mix II for a total reaction volume of 5 μl and amplification was performed on a ABI 7900HT Fast Real-Time PCR system following manufacturers protocols for TaqMan assays. Data was analyzed using Sequence Detection Systems version 2.4.1 (Applied Biosystems). GeNorm was used to analyze candidate reference genes according to average expression stability as described previously (Vandesompele et al., 2002), and the normalization factor derived from the two most stable genes was chosen for normalization. Normalized gene expression data was analyzed using repeated measures ANOVA with the transcripts as the repeated measure and genotype and treatment as independent factors, followed by Fisher's LSD for post hoc analysis (n=5 per group).

Other statistical analyses

For analyzing the effects of TRO compounds on body weight over the 3 months treatment period a $2 \times 2 \times 4$ repeated measures ANOVA was used, followed by Fisher's LSD. For motor performance and coordination, 2×5 repeated measures ANOVA followed by Fisher's LSD were used to compare mean trial scores for errors per step, time to traverse, and number of steps across trials, genotypes and drug treatment. Spontaneous activity in the cylinder was analyzed using a 2×2 randomized design ANOVA followed by Fisher's LSD to compare mean number of rears, forelimb and hindlimb steps, and time spent grooming across

genotype and drug treatment. For the pole test, groups were compared using Mann-Whitney U. For the buried pellet test, Fisher exact test was used for frequency analysis of mice above or below the median performance of wildtype mice treated with vehicle, and group medians were compared using Mann-Whitney U; in both cases one-tailed tests were used for drug effects in transgenic mice, where there is no possibility to detect a further increase in olfaction deficit. 4×2 repeated measures ANOVA followed by Holm-Sidak test was used for analysis of the number and percentage area covered by proteinase K-resistant alpha-synuclein aggregates. The hypergeometric test (phyper function in R) was used to assess significance of overlaps between 2 gene lists. All analyses were conducted with GB-STAT software (Dynamic Microsystems, Inc. Silver Spring, MD) or Sigma Plot software (Systat, 2011) for PC. The level of significance was set at $p < 0.05$.

Results and Discussion

Brain levels of cholesterol oximes and effects on general health

TRO40303 and TRO19622 were given to wildtype and Thy1-aSyn male mice in formulated rodent food pellets. There were no differences in food intake between mice treated with control diet or TRO compounds (Table S1).

TRO19622 at 1280 mg or 60 mg per kg food pellets resulted in ~8.5 μM and ~1 μM brain concentration, respectively (see table S2 for μg/g). TRO40303 at 700 mg or 70 mg per kg food pellets resulted in ~2.25 μM and ~0.25 μM brain concentration, respectively (see table S2 for μg/g). These brain concentrations were similar after 1, 2 or 3 months of continuous treatment, supporting stable brain concentrations over the course of the treatment and during behavioral testing. For both compounds a brain concentration above 1.5 μM (achieved for both high dosage treatment groups) is considered pharmacologically active based on previous in vitro studies (Bordet et al., 2007; Schaller et al., 2010). Accordingly, the drug regimen used in this study achieved, as intended, pharmacologically active concentrations in brain with the high dose of each compound and inactive dosage with the low dose. Behavioral and pharmacological studies were conducted with both doses and transcriptome analyses with the high doses only. Plasma concentrations were ~4 fold higher than brain concentration (Table S2).

Treatment with TRO19622 or TRO40303 for 3 months did not lead to any side effects, signs of distress or decrease of general health condition in wildtype and Thy1-aSyn transgenic mice, confirming previous observations (Bordet et al., 2007; Schaller et al., 2010). As described previously, weight gain in transgenic mice was slightly lower compared to wildtype mice (Fleming et al., 2004) (Table S3). TRO19622 significantly increased weight gain in wildtype (low dose) and transgenic (high and low dose) mice. In transgenic mice the body weight was positively correlated to the plasma level of TRO19622 low dose (0.87 $p < 0.05$). This suggests that TRO19622 has beneficial effects on the lower weight gain in transgenic mice. TRO40303 significantly decreased weight gain in wildtype and transgenic mice. However, TRO40303 fed mice did not show any signs of toxicity or decreased/increased food intake compared to mice on control diet. Body temperatures did not differ between genotypes or drug treatment groups (not shown).

Gene expression network analysis reveals a strong effect of TRO40303 on gene expression

TRO compounds are cytoprotective in a broad range of diseases including neurodegenerative diseases and cardiovascular dysfunction. Administration of the high dose of TRO19622 changed the expression levels of 1328 probes (representing 1295 genes) in wildtype (673 down, 655 up) and of 1670 probes (representing 1612 genes) in Thy1-aSyn mice (843 down, 827 up), with 122 probes (representing 121 genes) overlapping between wildtype and Thy1-aSyn mice (over-representation factor 1.4, p < 6.585e-05, hypergeometric test). High dose TRO40303 changed expression levels of 2918 probes (representing 2726 genes) in wildtype (1304 down, 1614 up) and of 1715 probes (representing 1640 genes) in Thy1-aSyn mice (820 down, 895 up) with 412 probes (representing 392 genes) overlapping between wildtype and Thy1-aSyn mice (over-representation factor 2.1 p < 2.319e-53). There was a significant overlap of transcriptional changes p<0.05 for both compounds (142 probes, Over-Representation factor: 1.3, p < 0.002). Despite different mechanisms of action (Bordet et al., 2007; Schaller et al., 2010) both compounds target mitochondria and have similar neuroprotective effects. Therefore, we focused on the transcripts that were strongly affected by both compounds and analyzed overlapping changes with a minimum log2-transformed fold change of 0.2 and a p-value <0.05 in wildtype mice. This strategy identified seventeen upregulated probes (representing 16 genes) (Over-Representation factor: 7.4 p < 1.442e-10) and 16 downregulated probes (representing 16 genes) (Over-Representation factor: 26.0 p < 3.945e-19) (Table S4). Overlapping transcripts include glutaredoxin (*Glcx2,* upregulated), a glutathione-dependent oxidoreductase that facilitates the maintenance of mitochondrial redox homeostasis upon induction of apoptosis by oxidative stress (Enoksson et al., 2005; Ferri et al., 2010; Nagy et al., 2008; Wu et al., 2010).

In order to functionally organize gene expression changes in our dataset, we first used weighted gene co-expression network analysis (WGCNA, (Zhang and Horvath, 2005)) a method in which the co-expression network is based on topological overlap between genes and considers the correlation of two genes with each other and the degree of their shared correlations within the network. WGCNA clusters functionally related transcripts into modules in an unsupervised manner based on the expression pattern across all samples. The result of clustering can be viewed as a dendrogram (Fig. 2A), in which each branch corresponds to a group of co-expressed genes (a module) that is designated a color and a number and will be referred to by its color for the rest of this manuscript. We condensed the gene expression pattern within a module to a 'module eigengene' (ME), which is a weighted summary of gene expression in the module and can be correlated to traits. The relationships between genes within modules can be identified, and follow up analyses can focus on hub genes (genes with highest connectivity in the module) and corresponding pathways driving gene expression changes without any a priori assumptions about gene function.

WGCNA grouped genes in 19 discrete modules (clustering shown in Fig 2B). Pearson correlation of these modules to treatment showed that TRO40303 administration was most significantly correlated to modules (Fig 2C). We selected the 4 modules most highly correlated to the administration of TRO40303 in wildtype and Thy1-aSyn mice (positively

correlated orange, tan and gold4 module, negatively correlated seagreen module). The tan, gold4 and the orange module are closely related as shown by cluster analysis of Fig 2B. We then annotated the modules with gene ontology (GO) to highlight main biological functions.

The tan ME (180 genes) is positively correlated to TRO40303 administration in both wildtype and Thy1-aSyn mice (correlation coefficient 0.42 p=0.01 in wildtype, 0.38 p=0.02 in Thy1-aSyn mice; Fig 3A). GO showed enrichment for genes encoding cytoplasmic proteins, intracellular organelles, intracellular protein transport, phosphorylation and other protein modifications (Table S5). This module is also enriched for genes involved in vesicle fusion (*Snap29, Stx7, Abl2*), vesicle-mediated transport (*Cadps, App, Stx7, Napg, Lrp11, Bcap29, Sar1b, Rhobtb3*), endosome (*Chmp2a, Lamp2, Stx7, Ndfip2, Stam, Cd164*) and neuron projection (*Tnfrsf21, App, Ppm1a, Abi2, Cask, Pygb*). A trend for enrichment (p<0.1) is present for negative regulation of apoptosis (*Atg5, Eef1a2, Prdx2, Glo1, Ube2b*) and mitochondrion outer membrane (*Acsl4, Vdac2, Acsl3*). The top 10 hub genes of this module are *Rnf11, Atf2, Laptm4a, Ppm1a, Ndfip1, Armcx3, Kbtbd2, App, Mrps33, Usp22*. Importantly, this module also contains Ddc, aromatic-L-amino-acid decarboxylase. This protein catalyzes the decarboxylation of L-3,4-dihydroxyphenylalanine (DOPA) to dopamine and L-5-hydroxytryptophan to serotonin (Siow and Dakshinamurti, 1990). The presence of this transcript supports the specificity of the analysis for dopaminergic neurons and its positive correlation to TRO40303 administration suggests an increase in dopamine synthesis.

The orange ME (43 genes) is positively correlated to TRO40303 administration in both wildtype and Thy1-aSyn mice (correlation coefficient 0.42 p=0.01 in wildtype, 0.35 p=0.03 in Thy1-aSyn mice; Fig 3B) and related to the tan module (cluster analysis in Fig 2B). GO (Table S6) showed enrichment for genes encoding cytoplasmic proteins and phosphoproteins as well as enzymatic functions that involve acetylation (*Clns1a, Satb1, Bclaf1, Ndufa9, Ak3, Prdx2, Ctnna1, Prdx1, Sacm1l, Pja2, Ppia, Prkar1a, Ubc, Stk39, Ranbp1, Srp9*) and ubiquitin conjugation (*Satb1, Gpr158, Ppia, Stmn2, Ubc, Ctnna1*). This module is further enriched for thioredoxin peroxidase activity (*Prdx1, Prdx2*) and for genes involved in programmed cell death (*Bclaf1, Ubc, Rrm2b, Prdx1, Gch1*). The top 10 hub genes of this module are *Sacm1l, Gap43, Bclaf1, Arl6ip1, Ndufa9, Ppia, Gpr158, Srp9* and *Ghitm*. Gch1 (GTP cyclohydrolase 1) is a critical enzyme for dopaminergic neurotransmission because it catalyzes the synthesis of the cofactor for TH, the rate-limiting enzyme of dopamine synthesis.

The gold4 ME (214 genes) is positively correlated to TRO40303 administration in both wildtype and Thy1-aSyn mice (correlation coefficient 0.45 p=0.005 in wildtype, 0.26 p=0.1 in Thy1-aSyn mice; Fig 3C) and related to the tan and orange module (Fig 2B). Similar to the orange ME, GO (Table S7) showed enrichment for cytoplasmic proteins, acetylation and phosphoproteins. In addition, this module has enrichment for mitochondrial genes (*Uqcrc1, Timm17a, Atp5b, Cs, Ndufa7, Bckdhb, Cyc1, Bcl2l2, Vdac3, Timm8b, Hagh, Slc25a11, Slc25a14, Kif1b, Ppm1k, Atp5c1, Rhot2, Elovl6, Pdha1, Hspa9*). Due to the enrichment in mitochondria related genes, this module is also enriched in transcripts associated with neurodegenerative diseases known to involve mitochondrial function, e.g. Parkinson's disease (*Uqcrc1, Atp5b, Slc6a3, Cyc1, Ndufa7, Atp5c1, Vdac3*), Alzheimer's disease

(*Uqcrc1, Atp5b, Cyc1, Ndufa7, Ppp3r1, Atp5c1, Calm2*) and Huntington's disease (*Uqcrc1, Atp5b, Cyc1, Ndufa7, Atp5c1, Vdac3*). The top 10 hub genes in this module are *Nsg2, Fbxo25, Atp6v1b2, Kifap3, Tmem85, Fbxl3a. Eef1a1, Kif5a, Prnp.* The association of TRO40303 with this module is compatible with the known effects of the drug on mitochondrial function.

The seagreen ME (72 genes) is negatively correlated to TRO40303 administration in both wildtype and Thy1-aSyn mice (correlation coefficient −0.43 p=0.008 in wildtype, −0.36 p=0.03 in Thy1-aSyn mice; (Fig 3D), meaning that expression of genes in this module is low in mice treated with TRO40303 compared to control or TRO19622 treated animals. GO (Table S8) showed an enrichment for LIM (Lin-11 Isl-1 Mec-3) domain related genes (*Lims1, Tgfb1i1, Csrp2*), as well as for genes involved in negative regulation of potassium ion transport, in negative regulation of cellular, developmental and multicellular organismal processes, in negative regulation of synaptic transmission and transmission of nerve impulse (*Stambp, Hhex, Sema3f, Pim1, Stxbp1, Nos3, Vax1, Tgfb1i1, Htr2a*). Furthermore, this module is enriched for genes related to the wnt receptor signaling pathway (*Hhex, Wnt5b, Tgfb1/1*). The top 10 hubgenes in the seagreen module are *Piwil1, Mbip, Zfp36l2, Tnpo2, 4930524e20rik, Slc13a3, Ian1, Psca, Echdc2, Olfr139*. Low expression of these genes in response to TRO40303 may indicate that gene expression of these negative regulators is blocked by the compound or its downstream effects, suggesting a beneficial shift of cellular processes.

Pathway analysis of cholesterol oximes effects reveals potential mechanism for cytoprotection

Guided by the networks identified in unbiased WGCNA we identified specific pathways robustly affected by the TRO compounds in dopaminergic neurons by focusing our analysis on differential transcript regulation with a p-value threshold of <0.005 and/or a minimum log2-transformed fold change of 0.2, as well as high intensity (expression) levels in our dataset. Most of the changes fitting these criteria were observed after TRO40303 administration. Therefore, TRO40303 effects on specific pathways, with mention of similar effects induced by TRO19622 administration, are highlighted below, first in wildtype mice (Fig. 4) and then under disease condition in alpha-synuclein overexpressing Thy1-aSyn mice (Table 1).

TRO40303 shifts transcriptome towards cytoprotection—The cytoprotective effect of TRO40303 has been suggested to result from prevention of outer mitochondrial membrane permeablization by stabilization of mPTP with reduced release of pro-apoptotic factors and reduction of oxidative stress (Bordet et al., 2007; Gouarne et al., 2013; Schaller et al., 2010). A set of proteins is thought to contribute to mPTP, including TSPO, cyclophilin D and VDAC (Shoshan-Barmatz and Ben-Hail, 2011). TRO19622 binds to TSPO and VDAC (Bordet et al., 2007), whereas TRO40303 binds TSPO only (Schaller et al., 2010). However, Vdac1 and Vdac2 transcripts were increased in TRO40303-treated wildtype mice whereas TRO19622 had no effect on either Vdac or Tspo transcripts.

VDAC plays a role in the release of apoptosis inducers by interaction with Bcl-2 family proteins (Shoshan-Barmatz and Ben-Hail, 2011). TRO40303 upregulated expression of anti-apoptotic Bcl2 family member Bcl2l2 in wildtype mice. Both TRO compounds have also been described to reduce oxidative stress (Bordet et al., 2007; Schaller et al., 2010). TRO40303 increased expression of enzymes crucial for oxidative stress defense and cytoprotection under cell stress in wildtype mice, specifically heat shock 70kDa protein 9 (Hspa9, mortalin), heat shock protein 90kDa alpha (Hsp90ab1) (Aridon et al., 2011), cyclophilin A (or peptidylprolyl isomerase A, *Ppia*) (Choi et al., 2007), peroxiredoxin 1 and 2 (Prdx1, Prdx2), glutaredoxin 2 (Glrx2) and thioredoxin like chromosome 10 open reading frame 58 (C10orf58) (Murphy, 2011). The latter two transcripts are also upregulated by TRO19622. Lastly, transcripts for three physiologically cytoprotective proteins also known for their potential to induce neurodegenerative diseases when misfolded, were upregulated by TRO40303: prion protein (Prnp), amyloid beta (A4) precursor protein (App) and endogenous mouse-alpha-synuclein (Snca). Whereas the misfolded form of prion protein is neurotoxic, the properly folded prion protein has neuroprotective properties attributed to a decrease in calcium overload in response to different cell stressors, an effect that has also been seen after exposure of cells to TRO40303 (Peggion et al., 2011; Schaller et al., 2010). Similar to App (Corrigan et al., 2011) and Prnp, wildtype Snca is protective to nerve terminals due to its physiological role in synaptic function (Chandra et al., 2005). Importantly, TRO40303 also increases integral membrane protein 2B (*Itm2b*, or Bri2) which reduces formation of amyloid plaques by interfering with APP cleavage (Matsuda et al., 2011).

TRO40303 increases Pink1 and modulates expression of mitochondrial dynamic genes—TRO40303 increased PTEN-induced putative kinase 1 (*Pink1,* which, when mutated (PARK6) causes autosomal recessive PD, $p < 0.05$, log ratio 0.43) and trafficking protein, kinesin binding 1 (*Trak1* or *Milt1*) transcripts, while decreasing ras homolog gene family, member T2 (*Rhot2* or *Miro-2*) in wildtype mice. The three proteins encoded by these genes build a complex important for mitochondrial trafficking (Wang et al., 2011), and an increase of Pink1 together with a decrease of Rhot2 might facilitate the quarantine of mitochondria that are targeted by Pink1 for degradation. Interestingly, TRO40303 upregulates Drp1 mRNA (dynamin 1-like, *Dnm1l*). Deletion of Drp1 specifically in dopamine neurons in vivo resulted in the early loss of dopamine terminals in the caudate putamen and degeneration of cell bodies predominantly in the substantia nigra (Berthet et al., 2013). Thus, increased expression of Drp1 may contribute to the neuroprotective profile of TRO40303 in nigral dopamine neurons.

TRO40303 increased expression of CRE binding Atf2 and myotrophin—We then investigated the differential expression of major transcription factors that are robustly regulated in both genotypes. As one would expect, the genes found to be highly regulated by TRO40303 are present in modules significantly correlated to TRO40303 treatment as described above. Specifically the tan module (Atf2, App, Ddc, Vdac2, Cask and C10orf58), the orange module (Gap43, Prdx1, Ppia, Prdx2 and Gch1), and the gold4 module (Prnp, Chrna6, Bcl2l2, Itm2b, Hspa9, Dnm1l, Pcbd, Rhot2, Slc6a3, Mtpn) include a large number of our genes of interest.

Atf2 is the hub gene with the second highest correlation in a WGCNA module that is positively correlated to TRO40303 treatment, and this same module also includes *Ddc*, meaning that *Atf2* and *Ddc* expression are highly correlated. *Atf2* is highly upregulated by TRO40303, and slightly by TRO19622 in wildtype. *Atf2* has been shown to upregulate transcripts of dopamine synthesis (Suzuki et al., 2002) (see below).

TRO40303 increases transcription of key enzymes in dopamine synthesis—As indicated earlier, two enzymes critical for dopamine synthesis, dopa decarboxylase (*Ddc*) and GTP cyclohydrolase 1 (*Gch1*) are members of modules that are positively correlated to TRO40303 treatment. Interestingly, expression of all three enzymes necessary for dopamine synthesis: *Gch1*, *Th* and *Ddc, and key genes for transport:* dopamine transporter (*Slc6a3*, or *Dat*) and the vesicular monoamine transporter 2 (*Slc18a2,* or *Vmat2*) were highly upregulated ($p<0.005$) in wildtype mice treated with TRO40303 compared to controls. In fact, *Dat* and *Vmat2* are the genes with the highest upregulation of expression by TRO40303 in wildtype mice. The cholinergic receptor, nicotinic, alpha 6 (*Chrna6*), which facilitates dopamine release upon ligand binding (Drenan et al., 2010), is also highly upregulated in wildtype mice in response to TRO40303. The dopamine receptor D2 (*Drd2*), a large number of transmitter release related genes, and dopamine metabolizing cytoplasmic aldehyde dehydrogenase Aldh1a1 are regulated by TRO40303. Importantly, Aldh1a1 is specific for dopaminergic neurons of the ventral mesencephalon and is decreased in brains of PD patients (Anderson et al., 2011). In summary, our data suggests upregulation of transcription of key enzymes in dopamine synthesis, storage, transport, release and metabolism in wildtype mice treated with TRO40303.

TRO compounds are effective in alpha-synuclein overexpressing Thy1-aSyn mice—A majority of described effects of TRO compounds in wildtype mice are also present in alpha-synuclein overexpressing Thy1-aSyn mice (Table 1), e.g. upregulation of Prdx2, C10orf58, Vdac1, Vdac2 and Drp1 ($p<0.05$). TRO40303 might therefore be beneficial to dopaminergic neurons under condition of alpha-synuclein pathology, by increasing mitochondria-related cytoprotective pathways.

Similar to wildtype mice, TRO40303 significantly upregulated *Atf2* in Thy1-aSyn mice and increased expression of dopamine related transcripts: *Th* and *Ddc* were highly upregulated with $p<0.005$, whereas the upregulation of *Dat*, *Vmat2* and *Aldh1a1* bordered on significance ($p<0.1$). Therefore, increased transcription of dopamine related transcripts by TRO40303 is attenuated but still present under conditions of alpha-synuclein mediated pathology.

Validation of TRO40303 effects on dopamine related transcripts

We used qRT-PCR on non-amplified RNA from a new set (independent replicates) of laser captured dopaminergic neurons from wildtype and Thy1-aSyn mice administered control or TRO40303 diet to verify the increase of dopamine related transcripts present in our microarray data. *Slc6a3 (Dat), Ddc, Th* and *Slc18a2 (Vmat2)* transcripts were significantly increased by TRO40303 treatment in wildtype mice, confirming the robust effect on gene expression found in our WGCNA and differential gene expression analysis (Fig. 5A). In

Thy1-aSyn mice (Fig. 5B) compared to control (n=5) TRO40303 had less pronounced effects on transcripts compared to the results of our microarray data where control treated groups of both TRO compounds were merged to increase power for statistical analysis (n=10 for each control group).

Transcriptional dysfunction in Thy1-aSyn mice (transgene effect)

Alpha-synuclein overexpression disrupts transcription in the striatum of young Thy1-aSyn mice (Cabeza-Arvelaiz et al., 2011) and previous studies of substantia nigra pars compacta tissue in mice overexpressing alpha-synuclein under the tyrosine hydroxylase promoter showed extensive differences in genes involved in transcription or translation, as well as signal transduction (Miller et al., 2007). In mice over-expressing alpha-synuclein under the PDGF promoter (Yacoubian et al., 2008) changes were observed in a small number of genes at 3 months of age with increased alterations at 9 months. However, transcriptome studies have not been previously performed in dopaminergic neurons isolated by laser capture microdissection from the substantia nigra of alpha-synuclein over-expressing mice. Following analysis of TRO40303 and TRO19622 effects on wild-type and Thy1-aSyn mice, we asked whether TRO compounds affected the transcriptional dysfunction that results from alpha-synuclein overexpression in dopaminergic neurons of Thy1-aSyn mice.

At 3 months of age, prior to any loss of striatal dopamine which only occurs at 14 months of age in these mice (Lam et al., 2011), nigrostriatal dopaminergic neurons of Thy1-aSyn mice already showed extensive transcriptional dysregulation compared to wildtype littermates. 1125 probes (representing 1103 genes) showed different levels of expression in wildtype and Thy1-aSyn mice (575 down, 550 were up). The top 7 pathways are shown in Fig. 6 and genes are listed in Table S9. All of the affected pathways are major signaling pathways involved in stress response or cell death. Transcripts dysregulated in Thy1-aSyn mice include Bcl2 (B-cell CLL/lymphoma 2, up), Casp3 (caspase 3, up), Bax (Bcl2-associated X protein, up) and Nos2 (nitric oxide synthase 2, inducible, up), all genes implicated in mitochondrial dysfunction and oxidative stress. Key genes involved in axon guidance signaling (canonical pathway $p<0.05$, 33 out of 429 molecules) were downregulated, including Itga3 (integrin, alpha 3, down), Wnt7b (wingless-type MMTV integration site family, member 7b, down) and Sema5a (semaphorin 5A, down, implicated in PD risk (Maraganore et al., 2005)).

Based on functional annotation clustering, Yacoubian et al. (2008) found that genes involved in transcription and cell cycle regulation were predominantly altered in 9-month old mice overexpressing alpha-synuclein under the PDGF promoter. In agreement with these results, the top canonical pathways in our analysis (Fig. 6) include signaling pathways, which result in regulation of transcription (e.g. ERK/MAPK signaling) as well as cell cycle progression (PI2K/AKT Signaling). More pronounced transcriptome alterations towards cell stress response in the dopaminergic neurons of Thy1-aSyn mice (e.g. Myc Mediated Apoptosis Signaling and PTEN Signaling) compared to the PDGF mice, which only occasionally express alpha-synuclein in nigral neurons, are in line with their more extensive nigral alpha-synuclein pathology (Rockenstein et al., 2002).

TRO19622 and TRO40303 ameliorated transcriptional dysfunction in Thy1-aSyn mice

Axon guidance signaling, a top canonical pathway which was altered in 4 months old Thy1-aSyn mice, was significantly altered by TRO19622 ($p<0.05$, 42 out of 429 molecules) and by TRO40303 ($p<0.05$, 47 out of 429 molecules, top canonical pathway) in Thy1-aSyn mice. For TRO40303 the largest log ratios applied to upregulated genes involved in axon outgrowth, integrin activation and cytoskeletal-membrane organization (Sema4f, Dpysl2, Rassf5, Ephb2, Sdcbp, Crk, Wint5a). TRO19622 effects were less pronounced but similar (upregulation of Sema7a, Dpysl2, Ephb2, Ntng1).

The analysis of genes that are changed in transgenic compared to wildtype mice shows that TRO19622 affected 225 of these probes (representing 225 genes, 20%) in transgenic mice (Over-Representation factor: 3.1, $p < 1.427e-54$). Importantly all except one (*Notch4*) of these transcripts were normalized by the drug towards wildtype level, with 192 (85%) being no longer different in Thy1-aSyn compared to wildtype littermate mice after TRO19622 administration. TRO40303 affected 203 (representing 202 genes, 18%) of the probes that showed differences between transgenic and wildtype mice (Over-Representation factor: 2.7, $p < 3.522e-40$). Similar to the effect of TRO19622, a large proportion of these transcripts (192, 95%) were closer to wildtype expression levels after administration of TRO40303, with 180 of the 202 transcripts (89%) fully normalized in Thy1-aSyn mice administered the drug. 46 probes (representing 46 genes, Table S10) were significantly different between control treated wildtype and Thy1-aSyn mice, and affected by both compounds. This fraction represents 32% of all genes that are affected by both compounds. Prominent among these genes is *Itpr1* (inositol 1,4,5-trisphosphate receptor, type 1, or spinocerebellar ataxia 15) which is strongly expressed and among the most highly regulated genes in our dataset (log ration −0.31 control treated Thy1-aSyn versus wildtype, log ratio 0.56 Thy1-aSyn TRO19622 versus control, log ratio 0.42 Thy1-aSyn TRO40303 versus control). This intracellular channel mediates calcium release from the endoplasmic reticulum following stimulation by inositol 1,4,5-trisphosphate and functions as a center for signaling cascades.

In summary, alpha-synuclein overexpression results in dysregulation of gene expression in nigral dopaminergic neurons of young Thy1-aSyn mice. TRO compounds affected each 18–20% of the genes dysregulated in Thy1-aSyn mice. Importantly, the large majority (85–89%) of these effects resulted in normalization of gene expression towards levels observed in wildtype mice, supporting an amelioration of transcriptional dysregulation in Thy1-aSyn mice by both TRO compounds. 32% overlap of the effects of the two TRO compounds on transcriptional dysregulation support common mechanisms in the context of alpha-synuclein overexpression.

Effects of TRO compounds on alpha-synuclein induced behavioral and pathological deficits

At the very young age examined in this study, Thy1-aSyn mice exhibit deficits in a range of motor and non-motor behavior that precede by about 10 months the emergence of parkinsonism, which accompanies the loss of striatal DA observed at 14 (but not 10) months of age in this model (Chesselet et al., 2012; Lam et al., 2011). Deficits in the cylinder, the pole test and the challenging beam were not improved by either TRO compound (Tables

S11 and S12), suggesting that they are not related to aspects of alpha-synuclein induced pathology that may be ameliorated by the cholesterol oximes. This is not surprising since neither drug improved alpha-synuclein aggregation (Table S13). In fact, high doses of TRO19622 increased the surface area occupied by alpha-synuclein aggregates in the substantia nigra, and in one subregion, also increased their number (Table S13). Since this effect was not observed with TRO4303, which induces the strongest effects on transcriptome, it is unlikely that it is related to the effects of the cholesterol oximes on gene expression in nigro-striatal dopaminergic neurons. Unfortunately, visualization of alpha-synuclein aggregates requires the use of proteinase K, which precludes their evaluation specifically in dopaminergic neurons since the treatment would destroy possible markers of these neurons, such as TH. The role of aggregates at this early age is not clear as dopaminergic neuron toxicity is only apparent after more than 14 months and indeed aggregate formation may be a means of sequestering protein and a strategy to prevent misfolded protein toxicity as observed in other neurodegenerative diseases, such as Huntington's disease (Arrasate et al., 2004).

The high dose of TRO40303, which induced the most robust improvement of transcriptional alterations in Thy1-aSyn mice, improved their olfactory deficits (Fig. 8). Specifically, the fraction of transgenic mice able to find a buried food reward within the median time of wildtypes on control diet increased after administration of TRO40303 high dose compared to transgenics fed a control diet (Fig. 8), and Thy1-aSyn mice treated with TRO40303 high dose find the food reward faster compared to transgenics receiving control food (mean ± SEM time to find the buried food reward: wildtype/control: 127.1±28.81s, wildtype/TRO40303: 93.3±17.17s; Thy1-aSyn/control: 211.7±22.68s; Thy1-aSyn/TRO40303 159.5±25.81s; $p < 0.05$ Thy1-aSyn control versus TRO40303). The mechanism of olfactory deficits in PD patients and in alpha-synuclein over-expressing mice is not known but has been related to changes in neurogenesis (Fleming et al., 2008; Hoglinger et al., 2004; Marxreiter et al., 2009; Marxreiter et al., 2013; Winner et al., 2004; Winner et al., 2008), a mechanisms that could be improved by the cholesterol oxime, independently of any effect on alpha-synuclein aggregation. Intriguingly, TRO40303 also increased the number of footslips ("errors per step") on the challenging beam, an effect reminiscent of that induced at similar ages in Thy1-aSyn mice by dopaminergic agonists (Fleming et al., 2006). We interpret this pharmacological effect as reflecting the motor impairment caused by excess dopamine and altered dopamine signaling in the striatum (Chesselet et al., 2012; Fleming et al., 2006; Fredriksson et al., 1990; Oksman et al., 2009) since these young Thy1-aSyn mice have excess extracellular dopamine in the striatum and altered striatal synaptic response to dopamine agonists and antagonists, pointing towards alteration of D2 receptor modulation (Lam et al., 2011). A similar effect on errors per step in Thy1-aSyn mice was produced by TRO40303, which increased the level of several transcripts involved in dopamine synthesis, suggesting that it may further increase dopamine level to impair motor performance on the beam similarly to l-dopa and apomorphine, perhaps through a mechanism involving D2 autoreceptors (Beaulieu and Gainetdinov, 2011; Guatteo et al., 2013; Muller et al., 2004).

In conclusion, the cholesterol oxime TRO40303 and to a lesser extent, TRO19622, when administered chronically at pharmacologically effective doses to young wildtype and alpha-synuclein overexpressing mice produce a range of effects on gene expression in nigro-

striatal dopaminergic neurons that suggest an improvement of mitochondrial function and dopamine metabolism. While not interfering directly with alpha-synuclein pathology and its behavioral consequences, TRO40303 may increase the resistance of dopaminergic neurons to mitochondrial dysfunction and other mechanisms that eventually lead to their demise in PD. Although small deficits in mitochondrial functions have been detected in young Thy1-aSyn mice, these measurements do not have sufficient power to detect drug effects (Sarafian et al., 2013). More recently, our laboratory has been able to identify mitochondrial deficits in Thy1-aSyn mice with the seahorse apparatus and by Western Blotting, methods that were not included in the present study (Subramaniam and Chesselet, in preparation). The results presented here pave the way for future studies to assess the effects of cholesterol oximes on these parameters and to evaluate their ability to prevent the loss of striatal dopamine in older Thy1-aSyn mice to further evaluate their neuroprotective potential in PD.

Supplementary Material

Refer to Web version on PubMed Central for supplementary material.

Acknowledgments

Non-standard Abbreviations

PD	Parkinson's disease
TBS	Tris-buffered saline
TH	tyrosine hydroxylase
Thy1-aSyn	mice overexpressing human wildtype α-synuclein under the Thy-1 promoter

References

Anderson DW, et al. Functional significance of aldehyde dehydrogenase ALDH1A1 to the nigrostriatal dopamine system. Brain Res. 2011; 1408:81–7. [PubMed: 21784415]

Aridon P, et al. Protective role of heat shock proteins in Parkinson's disease. Neurodegener Dis. 2011; 8:155–68. [PubMed: 21212626]

Arrasate M, et al. Inclusion body formation reduces levels of mutant huntingtin and the risk of neuronal death. Nature. 2004; 431:805–10. [PubMed: 15483602]

Beaulieu JM, Gainetdinov RR. The physiology, signaling, and pharmacology of dopamine receptors. Pharmacol Rev. 2011; 63:182–217. [PubMed: 21303898]

Berthet A, et al. Mitochondrial fission in dopamine neurons. Neurosci Abstr. 2013 714.05/H11.

Bordet T, et al. Specific antinociceptive activity of cholest-4-en-3-one, oxime (TRO19622) in experimental models of painful diabetic and chemotherapy-induced neuropathy. J Pharmacol Exp Ther. 2008; 326:623–32. [PubMed: 18492948]

Bordet T, et al. Identification and characterization of cholest-4-en-3-one, oxime (TRO19622), a novel drug candidate for amyotrophic lateral sclerosis. J Pharmacol Exp Ther. 2007; 322:709–20. [PubMed: 17496168]

Cabeza-Arvelaiz Y, et al. Analysis of striatal transcriptome in mice overexpressing human wild-type alpha-synuclein supports synaptic dysfunction and suggests mechanisms of neuroprotection for striatal neurons. Mol Neurodegener. 2011; 6:83. [PubMed: 22165993]

Chandra S, et al. Alpha-synuclein cooperates with CSPalpha in preventing neurodegeneration. Cell. 2005; 123:383–96. [PubMed: 16269331]

Chesselet MF, et al. A progressive mouse model of Parkinson's disease: the Thy1-aSyn ("Line 61") mice. Neurotherapeutics. 2012; 9:297–314. [PubMed: 22350713]

Choi KJ, et al. Overexpressed cyclophilin A in cancer cells renders resistance to hypoxia- and cisplatin-induced cell death. Cancer Res. 2007; 67:3654–62. [PubMed: 17440077]

Coppola G. Designing, performing, and interpreting a microarray-based gene expression study. Methods Mol Biol. 2011; 793:417–39. [PubMed: 21913117]

Coppola G, et al. Gene expression study on peripheral blood identifies progranulin mutations. Ann Neurol. 2008; 64:92–6. [PubMed: 18551524]

Corrigan F, et al. The neuroprotective domains of the amyloid precursor protein, in traumatic brain injury, are located in the two growth factor domains. Brain Res. 2011; 1378:137–43. [PubMed: 21215734]

de Tassigny A, et al. Mitochondrial translocator protein (TSPO) ligands prevent doxorubicin-induced mechanical dysfunction and cell death in isolated cardiomyocytes. Mitochondrion. 2013; 13:688–97. [PubMed: 24121045]

Devi L, et al. Mitochondrial import and accumulation of alpha-synuclein impair complex I in human dopaminergic neuronal cultures and Parkinson disease brain. J Biol Chem. 2008; 283:9089–100. [PubMed: 18245082]

Drenan RM, et al. Cholinergic modulation of locomotion and striatal dopamine release is mediated by alpha6alpha4* nicotinic acetylcholine receptors. J Neurosci. 2010; 30:9877–89. [PubMed: 20660270]

Enoksson M, et al. Overexpression of glutaredoxin 2 attenuates apoptosis by preventing cytochrome c release. Biochem Biophys Res Commun. 2005; 327:774–9. [PubMed: 15649413]

Ferri A, et al. Glutaredoxin 2 prevents aggregation of mutant SOD1 in mitochondria and abolishes its toxicity. Hum Mol Genet. 2010; 19:4529–42. [PubMed: 20829229]

Fleming SM, et al. A pilot trial of the microtubule-interacting peptide (NAP) in mice overexpressing alpha-synuclein shows improvement in motor function and reduction of alpha-synuclein inclusions. Mol Cell Neurosci. 2011; 46:597–606. [PubMed: 21193046]

Fleming SM, et al. Early and progressive sensorimotor anomalies in mice overexpressing wild-type human alpha-synuclein. J Neurosci. 2004; 24:9434–40. [PubMed: 15496679]

Fleming SM, et al. Behavioral effects of dopaminergic agonists in transgenic mice overexpressing human wildtype alpha-synuclein. Neuroscience. 2006; 142:1245–53. [PubMed: 16934409]

Fleming SM, et al. Olfactory deficits in mice overexpressing human wildtype alpha-synuclein. Eur J Neurosci. 2008; 28:247–56. [PubMed: 18702696]

Fredriksson A, et al. MPTP-induced hypoactivity in mice: reversal by L-dopa. Pharmacol Toxicol. 1990; 67:295–301. [PubMed: 2077520]

Gouarne C, et al. Olesoxime protects embryonic cortical neurons from camptothecin intoxication by a mechanism distinct from BDNF. Br J Pharmacol. 2013; 168:1975–88. [PubMed: 23278424]

Guatteo E, et al. Dual effects of L-DOPA on nigral dopaminergic neurons. Exp Neurol. 2013; 247:582–94. [PubMed: 23481547]

Hardy J. Genetic analysis of pathways to Parkinson disease. Neuron. 2010; 68:201–6. [PubMed: 20955928]

Hoglinger GU, et al. Dopamine depletion impairs precursor cell proliferation in Parkinson disease. Nat Neurosci. 2004; 7:726–35. [PubMed: 15195095]

Johnson WE, et al. Adjusting batch effects in microarray expression data using empirical Bayes methods. Biostatistics. 2007; 8:118–27. [PubMed: 16632515]

Kamme F, et al. Single-cell laser-capture microdissection and RNA amplification. Methods Mol Med. 2004; 99:215–23. [PubMed: 15131340]

Konopka G, et al. Human-specific transcriptional regulation of CNS development genes by FOXP2. Nature. 2009; 462:213–7. [PubMed: 19907493]

Lam HA, et al. Elevated tonic extracellular dopamine concentration and altered dopamine modulation of synaptic activity precede dopamine loss in the striatum of mice overexpressing human alpha-synuclein. J Neurosci Res. 2011; 89:1091–102. [PubMed: 21488084]

Le Lamer S, et al. Translation of TRO40303 from myocardial infarction models to demonstration of safety and tolerance in a randomized Phase I trial. J Transl Med. 2014; 12:38. [PubMed: 24507657]

Lenglet T, et al. A phase II-III trial of olesoxime in subjects with amyotrophic lateral sclerosis. Eur J Neurol. 2014; 21:529–36. [PubMed: 24447620]

Lin MT, Beal MF. Mitochondrial dysfunction and oxidative stress in neurodegenerative diseases. Nature. 2006; 443:787–95. [PubMed: 17051205]

Loeb V, et al. The transgenic overexpression of alpha-synuclein and not its related pathology associates with complex I inhibition. J Biol Chem. 2010; 285:7334–43. [PubMed: 20053987]

Magalon K, et al. Olesoxime accelerates myelination and promotes repair in models of demyelination. Ann Neurol. 2012; 71:213–26. [PubMed: 22367994]

Maraganore DM, et al. High-resolution whole-genome association study of Parkinson disease. Am J Hum Genet. 2005; 77:685–93. [PubMed: 16252231]

Martin LJ, et al. The mitochondrial permeability transition pore regulates nitric oxide-mediated apoptosis of neurons induced by target deprivation. J Neurosci. 2011; 31:359–70. [PubMed: 21209222]

Marxreiter F, et al. Changes in adult olfactory bulb neurogenesis in mice expressing the A30P mutant form of alpha-synuclein. Eur J Neurosci. 2009; 29:879–90. [PubMed: 19291219]

Marxreiter F, et al. Adult neurogenesis in Parkinson's disease. Cell Mol Life Sci. 2013; 70:459–73. [PubMed: 22766974]

Matsuda S, et al. Maturation of BRI2 generates a specific inhibitor that reduces APP processing at the plasma membrane and in endocytic vesicles. Neurobiol Aging. 2011; 32:1400–8. [PubMed: 19748705]

Meurers BH, et al. Low dose rotenone treatment causes selective transcriptional activation of cell death related pathways in dopaminergic neurons in vivo. Neurobiol Dis. 2008

Miller RM, et al. Wild-type and mutant alpha-synuclein induce a multi-component gene expression profile consistent with shared pathophysiology in different transgenic mouse models of PD. Exp Neurol. 2007; 204:421–32. [PubMed: 17254569]

Muller T, et al. Worsened motor test performance following acute apomorphine injection in previously untreated patients with Parkinson's disease. J Neural Transm Suppl. 2004:79–87. [PubMed: 15354392]

Murphy MP. Mitochondrial thiols in antioxidant protection and redox signaling: distinct roles for glutathionylation and other thiol modifications. Antioxid Redox Signal. 2011; 16:476–95. [PubMed: 21954972]

Nagy N, et al. Overexpression of glutaredoxin-2 reduces myocardial cell death by preventing both apoptosis and necrosis. J Mol Cell Cardiol. 2008; 44:252–60. [PubMed: 18076901]

Nakamura K. alpha-Synuclein and mitochondria: partners in crime? Neurotherapeutics. 2013; 10:391–9. [PubMed: 23512373]

Oksman M, et al. Behavioural and neurochemical response of alpha-synuclein A30P transgenic mice to the effects of L-DOPA. Neuropharmacology. 2009; 56:647–52. [PubMed: 19084027]

Pankratz N, et al. Alpha-synuclein and familial Parkinson's disease. Mov Disord. 2009; 24:1125–31. [PubMed: 19412953]

Peggion C, et al. Possible role for Ca2+ in the pathophysiology of the prion protein? Biofactors. 2011; 37:241–9. [PubMed: 21698700]

Richter F, et al. Neurons express hemoglobin alpha- and beta-chains in rat and human brains. J Comp Neurol. 2009; 515:538–47. [PubMed: 19479992]

Rockenstein E, et al. Differential neuropathological alterations in transgenic mice expressing alpha-synuclein from the platelet-derived growth factor and Thy-1 promoters. J Neurosci Res. 2002; 68:568–78. [PubMed: 12111846]

Sarafian TA, et al. Impairment of mitochondria in adult mouse brain overexpressing predominantly full-length, N-terminally acetylated human alpha-synuclein. PLoS One. 2013; 8:e63557. [PubMed: 23667637]

Schaller S, et al. TRO40303, a new cardioprotective compound, inhibits mitochondrial permeability transition. J Pharmacol Exp Ther. 2010; 333:696–706. [PubMed: 20215409]

Schapira AH, et al. Mitochondrial complex I deficiency in Parkinson's disease. Lancet. 1989; 1:1269. [PubMed: 2566813]

Schapira AH, Jenner P. Etiology and pathogenesis of Parkinson's disease. Mov Disord. 2011; 26:1049–55. [PubMed: 21626550]

Shoshan-Barmatz V, Ben-Hail D. VDAC, a multi-functional mitochondrial protein as a pharmacological target. Mitochondrion. 2011; 12:24–34. [PubMed: 21530686]

Siow YL, Dakshinamurti K. Neuronal dopa decarboxylase. Ann N Y Acad Sci. 1990; 585:173–88. [PubMed: 2192610]

Stocchi F, Olanow CW. Obstacles to the development of a neuroprotective therapy for Parkinson's disease. Mov Disord. 2013; 28:3–7. [PubMed: 23390094]

Subramaniam SR, Chesselet MF. Mitochondrial dysfunction and oxidative stress in Parkinson's disease. Prog Neurobiol. 2013; 106–107:17–32.

Sunyach C, et al. Olesoxime delays muscle denervation, astrogliosis, microglial activation and motoneuron death in an ALS mouse model. Neuropharmacology. 2012; 62:2346–52. [PubMed: 22369784]

Suzuki T, et al. Identification of ATF-2 as a transcriptional regulator for the tyrosine hydroxylase gene. J Biol Chem. 2002; 277:40768–74. [PubMed: 12196528]

Vandesompele J, et al. Accurate normalization of real-time quantitative RT-PCR data by geometric averaging of multiple internal control genes. Genome Biol. 2002; 3:RESEARCH0034. [PubMed: 12184808]

Wang X, et al. PINK1 and Parkin target Miro for phosphorylation and degradation to arrest mitochondrial motility. Cell. 2011; 147:893–906. [PubMed: 22078885]

Winner B, et al. Human wild-type alpha-synuclein impairs neurogenesis. J Neuropathol Exp Neurol. 2004; 63:1155–66. [PubMed: 15581183]

Winner B, et al. Mutant alpha-synuclein exacerbates age-related decrease of neurogenesis. Neurobiol Aging. 2008; 29:913–25. [PubMed: 17275140]

Wu H, et al. Glutaredoxin 2 prevents H(2)O(2)-induced cell apoptosis by protecting complex I activity in the mitochondria. Biochim Biophys Acta. 2010; 1797:1705–15. [PubMed: 20547138]

Xiao WH, et al. Olesoxime (cholest-4-en-3-one, oxime): analgesic and neuroprotective effects in a rat model of painful peripheral neuropathy produced by the chemotherapeutic agent, paclitaxel. Pain. 2009; 147:202–9. [PubMed: 19833436]

Xiao WH, et al. Characterization of oxaliplatin-induced chronic painful peripheral neuropathy in the rat and comparison with the neuropathy induced by paclitaxel. Neuroscience. 2012; 203:194–206. [PubMed: 22200546]

Yacoubian TA, et al. Transcriptional dysregulation in a transgenic model of Parkinson disease. Neurobiol Dis. 2008; 29:515–28. [PubMed: 18191405]

Yang YM, et al. A small molecule screen in stem-cell-derived motor neurons identifies a kinase inhibitor as a candidate therapeutic for ALS. Cell Stem Cell. 2013; 12:713–26. [PubMed: 23602540]

Zhang B, Horvath S. A general framework for weighted gene co-expression network analysis. Stat Appl Genet Mol Biol. 2005; 4:Article17. [PubMed: 16646834]

Highlights

- cholesterol-oximes increase stress defense mRNAs in nigrostriatal dopaminergic neurons

- cholesterol-oximes increase dopamine-related mRNAs in nigrostriatal dopaminergic neurons

- alpha-synuclein over-expression induces transcriptome changes in nigrostriatal neurons

- cholesterol-oximes reverse a subset of these alpha-synuclein induced alterations
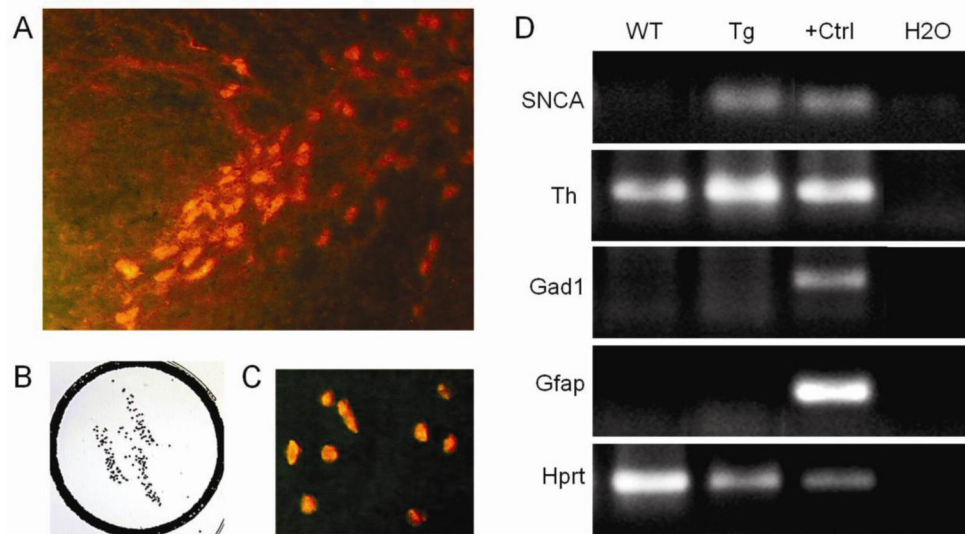
**Fig. 1. Transcriptome analysis on isolated dopaminergic neurons**
A, Dopaminergic neurons of the substantia nigra pars compacta labeled by TH immunofluorescence prior to LCM. B,C, captured TH-positive neurons (B by reverse light microscopy and C by fluorescent microscopy). D, Gel electrophoresis of PCR products from amplified mRNA of 500 nigral TH-positive neurons from wild-type (WT) and Thy1-aSyn transgenic (Tg) mice. As expected, human wildtype *alpha synuclein* (SNCA 68 bp) is expressed in samples of Thy1-aSyn mice only. Laser captured nigral neurons used for this analysis express *Th* (Th, ~200 bp) and the housekeeping gene *hypoxanthine guanine phosphoribosyl transferase* (Hprt, ~200 bp), but not *glutamic acid decarboxylase 1* (Gad1, gamma-aminobutyric acid (GABA)ergic neuron marker, ~200 bp) and *glial fibrillary acidic protein* (Gfap, glial cell marker, ~200 bp). Positive control (+Ctrl) for *Th*, *Hprt, Gad1*, and *Gfap* is cDNA from total mouse brain RNA and for *SNCA* total human brain RNA, negative control is water (H2O).
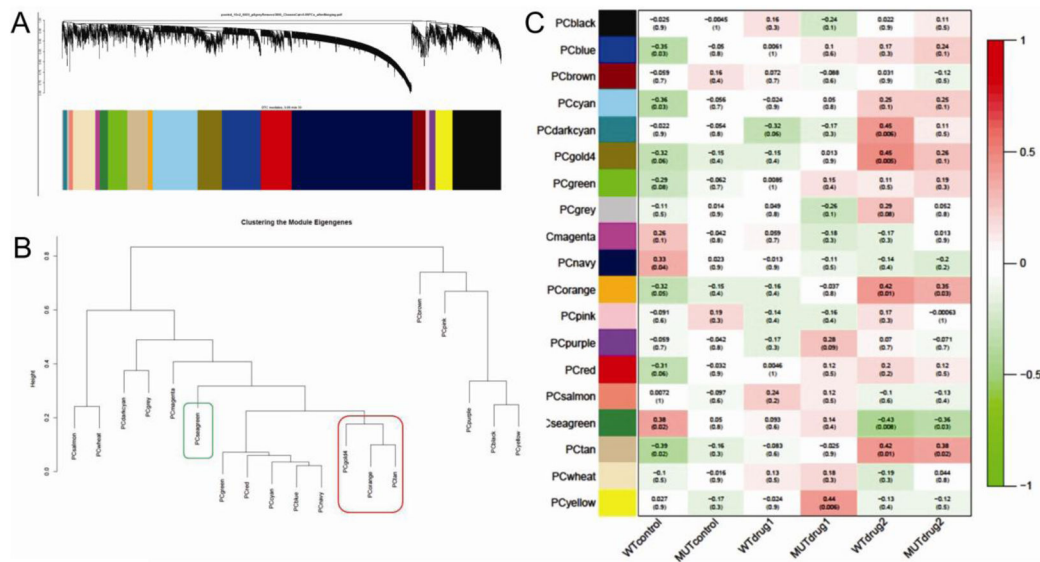
Fig. 2. Clustering of the module eigengenes by WGCNA and correlation to drug administration
A, dendrogram and resulting modules. B, clustering of module eigengenes. C, correlation of module eigengenes to drug administration (WT, wildtype; MUT, Thy1-aSyn; drug1, TRO19622; drug2, TRO40303. The gold4, orange and tan modules cluster (red box) and are positively correlated to TRO40303 administration. The seagreen module (green box) is negatively correlated to TRO40303 treatment.
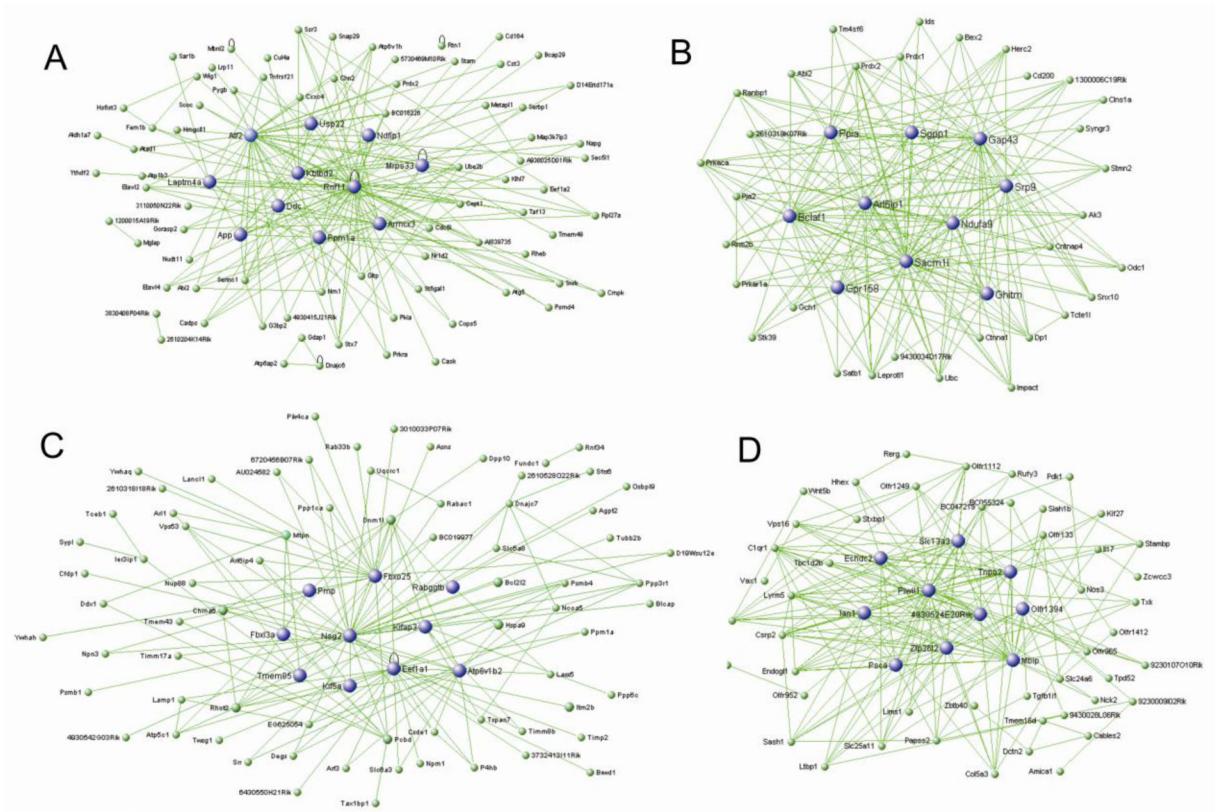
Fig. 3. Module significantly correlated to TRO40303 treatment
Hub genes in blue of the A Tan module, B orange module, C gold4 module, D seagreen
module. Green lines show correlation network.
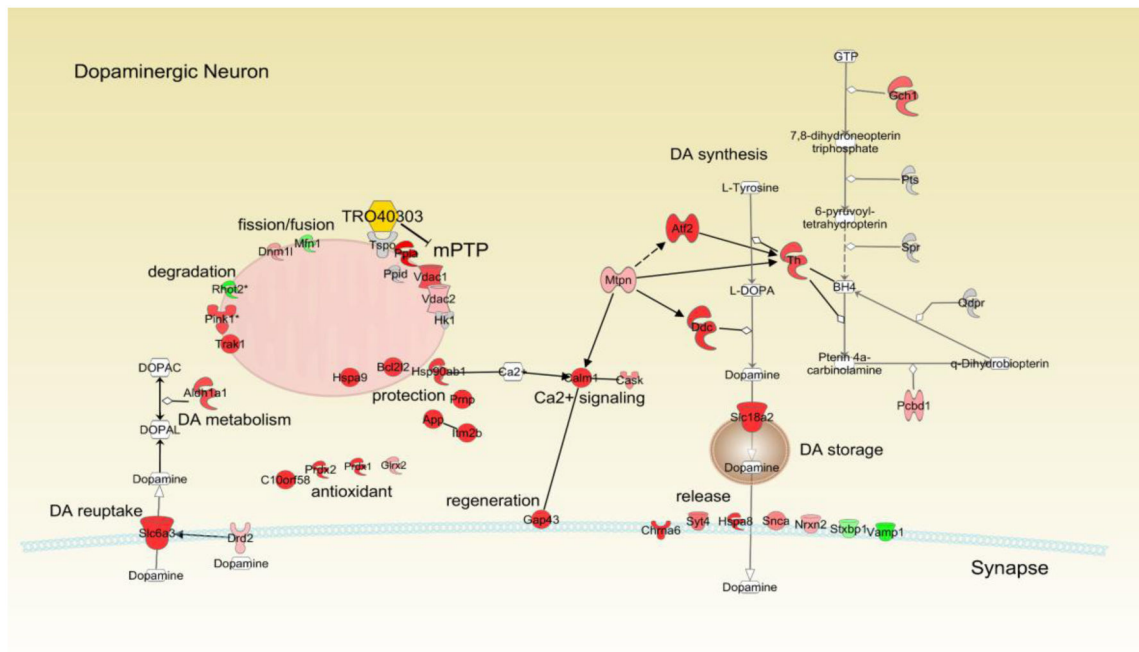
Fig. 4. Transcripts significantly regulated by TRO40303 in wildtype mice
Red indicates significant upregulation, and green significant downregulation, saturation of color shows the strength of the effect. Grey color indicates no change in expression. White color is used for chemicals apart from TRO40303 which is in yellow. Connections between genes indicate that binding occurs, arrows indicate that gene regulate each other's function or transcription. Some enzymatic reactions are indicated for dopamine related pathways (line ending in open trapezoids). See text for details.
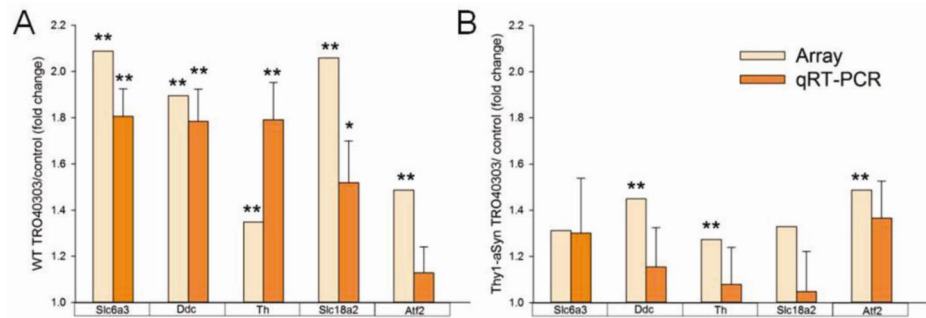
Fig. 5. Quantitative RT-PCR of dopamine related genes

differentially expressed in TRO40303 treated (A) wildtype (WT) and (B) Thy1-aSyn mice compared to respective WT or Thy1-aSyn controls. Fold changes and significance for array data (n=5–10 per group) are given for comparison (see also Table 1). Mean fold changes ± SEM, *p<0.05, **p<0.01, repeated measures ANOVA and Fisher LSD for qRT-PCR (n=5 per group).
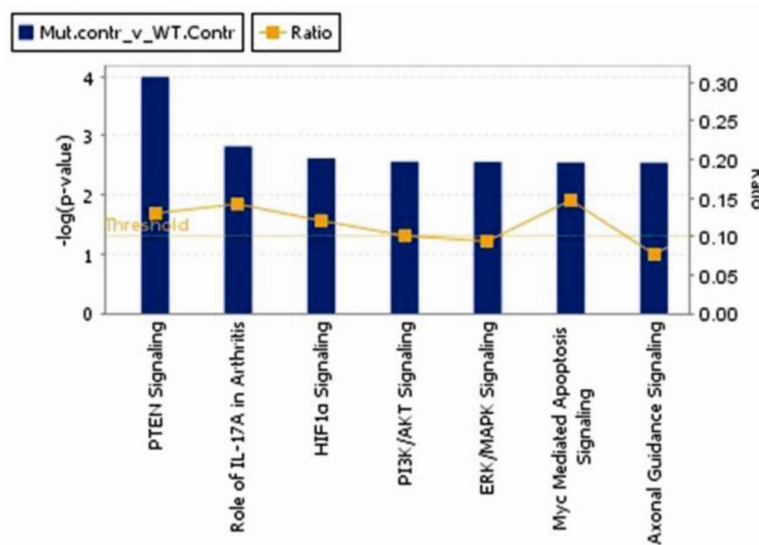
Fig. 6. Top 7 canonical pathways (p<0.05)
for genes differentially expressed in dopaminergic neurons of wildtype versus Thy1-aSyn mice. The yellow horizontal line marks the threshold for significance in the −log(p-value) visualized as blue bars. The yellow curve is the ratio of genes in the dataset that are in the respective canonical pathway and all genes in this pathway (IPA).
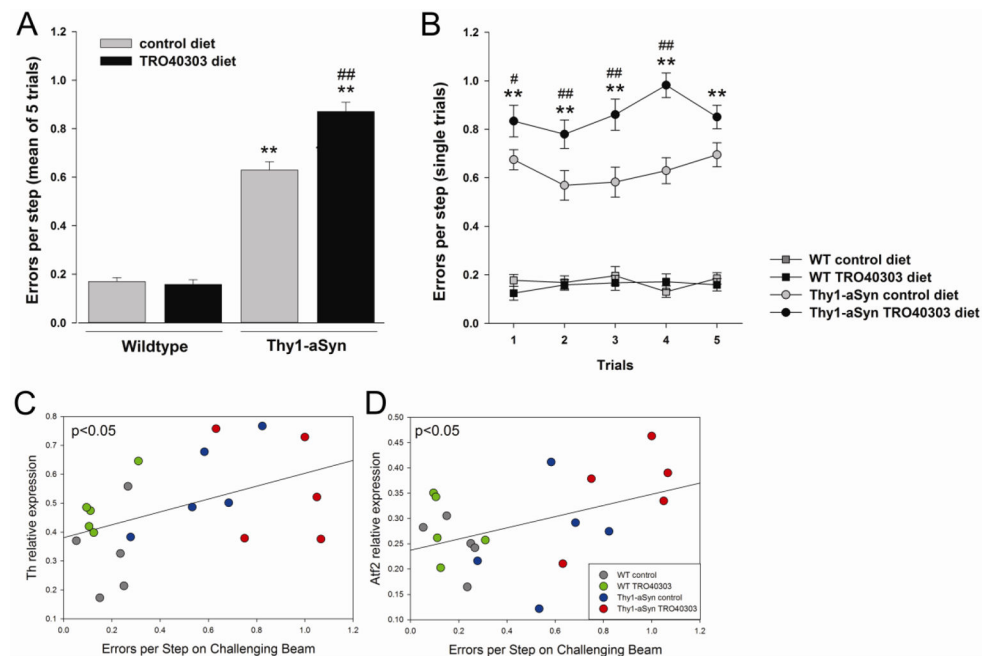
Fig. 7. Effect of TRO40303 on motor skills in the challenging beam test

Errors per step as mean of 5 trials (A) and over the 5 single trials (B) on the challenging beam following 3 months of treatment with TRO40303 (high dose) compared to respective control diet. Mean ± SEM; **p<0.01 Thy1-aSyn compared to WT control diet (transgene effect), # p<0.05, ## 0.01 Thy1-aSyn TRO40303 compared to Thy1-aSyn control diet (drug effect), (2×5 ANOVA, Fisher's LSD; n=16–20 per group). Upregulation of transcription of *Th* (C) and *Atf2* (D) correlate to Errors per Step (trial 4) in the respective groups treated with high dose of TRO40303 (Pearson correlation, p<0.05, n=5 per group).
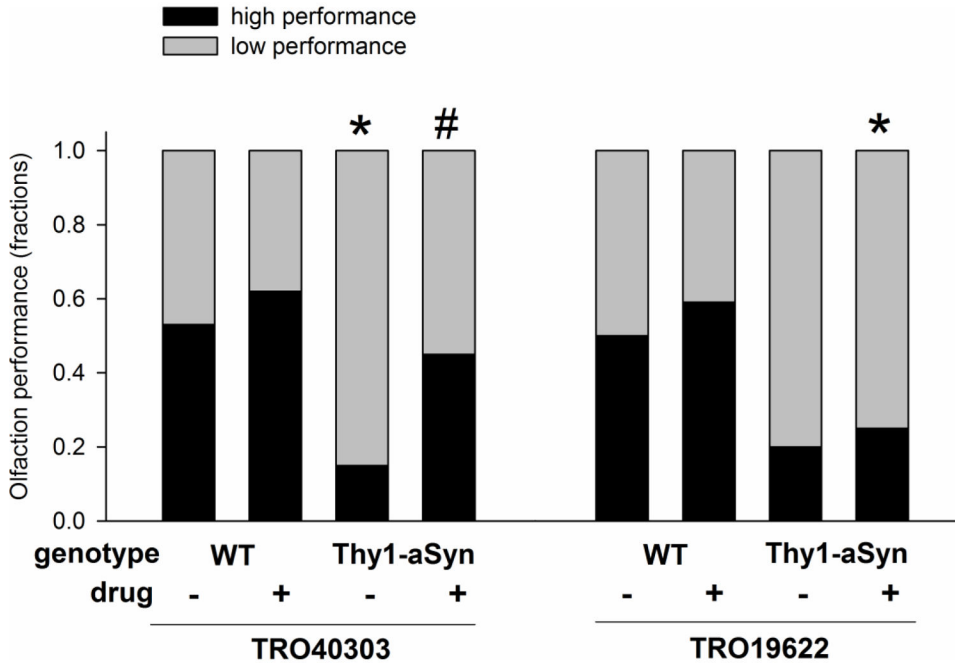
Fig. 8. TRO40303 improved olfaction deficits of Thy1-aSyn mice
Time to find a buried food reward was measured in wildtype (WT) and Thy1-aSyn mice treated with TRO40303 (n=20–21) or TRO19622 (n=17–21) at the high dose and compared to respective control (n=20 each). The fraction of mice that performed above (faster) than the median of wildtype (WT) mice administered control diet are defined as high performers and shown here by the black bars. Thy1-aSyn mice on control diet show low performance on this test compared to WT (*p<0.05, 2-tailed Fisher exact test). More Thy1-aSyn mice treated with TRO40303 reached high performance compared to control treated transgenics (#p<0.05; 1-tailed Fisher exact test).

Table 1

Effect of TRO40303 on gene expression in wildtype and Thy1-aSyn mice (genes selected from pathway analysis, see text for discussion). "Intensity %" is the percentile of intensity (expression) level of the probe compared to all intensities in the study (100% being the highest expression level). N=5 per group.

Gene symbol	Gene name	Accession	Wildtype TRO40303/control		Thy1-aSyn TRO40303/control		control Thy1-aSyn/Wildtype		TRO40303 Thy1-aSyn/Wildtype	
			log ratio (Intensity %)	p-value	log ratio	p-value	log ratio	p-value	log ratio	p-value
Aldh1a1	aldehyde dehydrogenase 1 family, member A1	NM_013467	0.427 (99)	0.02623	0.38	0.05508	0.056	0.72684	0.009	0.96694
App	amyloid beta (A4) precursor protein	NM_007471	0.599 (93)	7.80E-04	0.517	0.00435	0.052	0.7157	−0.031	0.86835
Atf2	activating transcription factor 2	NM_001025093	0.572 (91)	2.00E-04	0.572	0.00031	0.036	0.76184	0.037	0.81763
Bcl2l2	BCL2-like 2	NM_007537	0.482 (95)	4.00E-05	0.243	0.02981	0.023	0.79932	−0.217	0.07671
C10orf58	chromosome 10 open reading frame 58	NM_027464	0.511 (96)	0.00414	0.428	0.0012	0.02	0.89124	−0.063	0.74553
Calm1	calmodulin 1	NM_007590	0.497 (99)	0.01001	0.302	0.1206	0.121	0.44888	−0.074	0.72562
Cask	calcium/calmodulin-dependent serine protein kinase (MAGUK family)	NM_009806	0.28 (95)	0.02134	0.273	0.03048	−0.052	0.61043	−0.059	0.66228
Chrna6	cholinergic receptor, nicotinic, alpha 6	NM_021369	0.5 (95)	1.00E-05	0.153	0.12827	0.143	0.08842	−0.204	0.06924
Slc6a3	solute carrier family 6 (neurotransmitter transporter, dopamine), member 3	NM_010020	1.062 (100)	0	0.392	0.06056	0.207	0.22777	−0.463	0.04674
Ddc	dopa decarboxylase (aromatic L-amino acid decarboxylase)	NM_016672	0.922 (99)	1.00E-05	0.535	0.00499	0.061	0.68118	−0.326	0.1076
Dnm1l	dynamin 1-like	NM_001025947	0.241 (88)	0.00225	0.215	0.0077	0.009	0.88777	−0.017	0.84099
Drd2	dopamine receptor D2	NM_010077	0.155 (81)	0.01853	0.102	0.12639	0.012	0.82641	−0.041	0.57591
Gap43	growth associated protein 43	NM_008083	0.481 (98)	0.00407	0.49	0.00481	0.146	0.28746	0.155	0.39499
Gch1	GTP cyclohydrolase 1	NM_008102	0.368 (96)	0.00163	0.163	0.15452	0.028	0.7664	−0.177	0.16224
Glrx2	glutaredoxin 2	NM_023505	0.212 (90)	0.01897	−0.042	0.64282	0.126	0.10159	−0.129	0.20445
Hk1	hexokinase 1	NM_010438	−0.027 (49)	0.29118	0.063	0.02223	−0.04	0.0801	0.051	0.09171
Hsp90ab1	heat shock protein 90kDa alpha (cytosolic), class B member 1	NM_008302	0.478 (98)	0.00111	0.27	0.06162	−0.041	−0.057	0.55081	0.11623
Hspa8	heat shock 70kDa protein 8	NM_031165	0.766 (100)	4.40E-04	0.293	0.16163	−0.03	0.86035	−0.503	0.03334
Hspa9	heat shock 70kDa protein 9 (mortalin)	NM_010481	0.522 (99)	1.40E-04	0.152	0.23978	0.174	0.10755	−0.196	0.17225
Itm2b	integral membrane protein 2B	NM_008410	0.622 (98)	5.00E-05	0.406	0.00636	0.134	0.25831	−0.082	0.59847
Mfn1	mitofusin 1	NM_024200	−0.275 (99)	0.02566	−0.282	0.02798	−0.141	0.17696	−0.147	0.2866
Mtpn	myotrophin	NM_008098	0.19 (86)	0.01596	0.241	0.00399	−0.01	0.8761	0.041	0.64103

Gene symbol	Gene name	Accession	Wildtype		Thy1-aSyn		control		TRO40303	
			TRO40303/control		TRO40303/control		Thy1-aSyn/Wildtype		Thy1-aSyn/Wildtype	
			log ratio (Intensity %)	p-value	log ratio	p-value	log ratio	p-value	log ratio	p-value
Nrxn2	neurexin 2	NM_020253	0.203 (84)	0.00165	0.061	0.32906	0.079	0.13593	−0.064	0.36132
Pcbd	pterin-4 alpha-carbinolamine dehydratase/dimerization cofactor of hepatocyte nuclear factor 1 alpha	NM_025273	0.219 (83)	0.00369	0.121	0.1061	0.021	0.72644	−0.076	0.35314
Pink1	PTEN induced putative kinase 1	NM_026880	0.43 (97)	0.01813	−0.008	0.96462	0.205	0.18094	−0.233	0.25142
Ppia	peptidylprolyl isomerase A (cyclophilin A)	XM_122180.1	0.665 (99)	3.00E-05	0.431	0.00485	0.045	0.70935	−0.189	0.24113
Prdx1	peroxiredoxin 1	NM_011034	0.533 (98)	2.80E-04	0.217	0.12228	0.06	0.60162	−0.256	0.10027
Prdx2	peroxiredoxin 2	NM_011563	0.681 (98)	0.00239	0.36	0.00043	0.16	0.37775	−0.213	0.38011
Prnp	prion protein	NM_011170	0.543 (100)	0.00109	0.415	0.01296	−0.076	0.56553	−0.204	0.25251
Rhot2	ras homolog gene family, member T2	NM_145999	−0.603 (99)	0.00579	−0.274	0.20682	−0.222	0.21868	0.107	0.6542
Slc18a2	solute carrier family 18 (vesicular monoamine), member 2	NM_172523	1.042 (99)	6.00E-05	0.411	0.09034	0.18	0.36558	−0.451	0.09385
Snca	synuclein, alpha (non A4 component of amyloid precursor)	NM_009221	0.297 (99)	0.02418	0.386	0.00579	0.041	0.70605	0.13	0.37581
Stxbp1	syntaxin binding protein 1	NM_009295	−0.204 (60)	0.01203	−0.191	0.0227	−0.021	0.74899	−0.008	0.9246
Syt4	synaptotagmin IV	NM_009308	0.343 (95)	0.00158	0.249	0.0223	−0.046	0.60199	−0.14	0.23393
Th	tyrosine hydroxylase	NM_009377	0.431 (98)	6.00E-05	0.349	0.00116	0.064	0.43582	−0.018	0.86884
Trak1	trafficking protein, kinesin binding 1	NM_175114	0.475 (96)	0.00411	0.217	0.18571	0.11	0.41839	−0.149	0.4099
Tspo	translocator protein (18kDa)	NM_009775.2	−0.017 (11)	0.47227	0.059	0.02047	−0.047	0.02766	0.03	0.28101
Vamp1	Vesicle-associated membrane protein 1 (synaptobrevin 1)	NM_009496	−0.42 (95)	3.50E-04	−0.225	0.04851	−0.08	0.38825	0.115	0.34988
Vdac1	voltage-dependent anion channel 1	NM_011694	0.435 (97)	0.00209	0.307	0.03042	−0.002	0.98364	−0.13	0.39277
Vdac2	voltage-dependent anion channel 2	NM_011695	0.165 (86)	0.04675	0.264	0.00321	0.167	0.0209	0.266	0.00668